Title

Beta cyclodextrins bind, stabilize, and remove lipofuscin bisretinoids from retinal pigment epithelium

Journal

Proceedings of the National Academy of Sciences of the United States of America, 111(14)

ISSN

0027-8424

Authors

Nociari, Marcelo M
Lehmann, Guillermo L
Bay, Andres E Perez
et al.

Publication Date

2014-04-08

DOI

10.1073/pnas.1400530111

Peer reviewed

Beta cyclodextrins bind, stabilize, and remove lipofuscin bisretinoids from retinal pigment epithelium

Marcelo M. Nociari[a,1], Guillermo L. Lehmann[a], Andres E. Perez Bay[a], Roxana A. Radu[b], Zhichun Jiang[b], Shelby Goicochea[a], Ryan Schreiner[a], J. David Warren[c], Jufang Shan[d], Ségolène Adam de Beaumais[e], Mickaël Ménand[e], Matthieu Sollogoub[e], Frederick R. Maxfield[c], and Enrique Rodriguez-Boulan[a,1]

[a]Margaret Dyson Vision Research Institute, [c]Department of Biochemistry, and [d]Department of Physiology, Weill Cornell Medical College of Cornell University, New York, NY 10065; [b]Stein Eye Institute, Department of Ophthalmology, University of California, Los Angeles, CA 90095; and [e]Sorbonne Universités, Université Pierre et Marie Curie Paris 06, Centre National de la Recherche Scientifique, Unité Mixte de Recherche 8232, Institut Parisien de Chimie Moléculaire, 75005 Paris, France

Edited by Janet R. Sparrow, Columbia University, New York, NY, and accepted by the Editorial Board February 27, 2014 (received for review January 14, 2014)

Accumulation of lipofuscin bisretinoids (LBs) in the retinal pigment epithelium (RPE) is the alleged cause of retinal degeneration in genetic blinding diseases (e.g., Stargardt) and a possible etiological agent for age-related macular degeneration. Currently, there are no approved treatments for these diseases; hence, agents that efficiently remove LBs from RPE would be valuable therapeutic candidates. Here, we show that beta cyclodextrins (β-CDs) bind LBs and protect them against oxidation. Computer modeling and biochemical data are consistent with the encapsulation of the retinoid arms of LBs within the hydrophobic cavity of β-CD. Importantly, β-CD treatment reduced by 73% and 48% the LB content of RPE cell cultures and of eyecups obtained from *Abca4-Rdh8* double knock-out (DKO) mice, respectively. Furthermore, intravitreal administration of β-CDs reduced significantly the content of bisretinoids in the RPE of DKO animals. Thus, our results demonstrate the effectiveness of β-CDs to complex and remove LB deposits from RPE cells and provide crucial data to develop novel prophylactic approaches for retinal disorders elicited by LBs.

aging | retinopathy | lipofuscinosis | residual bodies

The retinal pigment epithelium (RPE), strategically situated between the neural retina and the choroid blood vessels, is essential for photoreceptor (PR) function. It recycles vitamin A, which is required for the visual cycle and clears debris generated by the circadian shedding of PR outer segments (1, 2). Each RPE cell phagocytoses and digests the material produced by 30–50 overlying PRs, which shed 10% of their mass daily. The intense and continual phagocytic activity of RPE cells results in the progressive accumulation of indigestible products or "lipofuscin" in their lysosomal compartment (3, 4). Unlike lipofuscins found in other body tissues, which are composed mainly of protein, RPE lipofuscin consists predominantly of lipid-bisretinoids and only 2% protein (5). Lipofuscin bisretinoids (LBs) are vitamin A-derived side products of the visual cycle. Light converts 11-*cis*-retinal (11CR), the visual pigment chromophore, into all-*trans*-retinal (ATR), which is immediately flipped by the ATP-binding cassette transporter 4 (*Abca4*) transporter from the lumen of the outer segment discs to the cytoplasm, where it is reduced to inert all-*trans*-retinol by retinol dehydrogenase 8 (*Rdh8*), in mice (6, 7). Small fractions of 11CR and ATR are converted into N-retinylidine-N-ethanolamine (A2E) and other less abundant bisretinoids, which once accumulated in the lysosomes of RPE cells are refractory to all known lysosomal hydrolases (8, 9). The concept that LB accumulation causes retinal degeneration is supported by in vitro and in vivo data that show that excessive LBs are toxic for cultured RPE cells (10, 11), that photoreceptors overlying A2E-laden RPE are more prone to degeneration (12) and that excessive accumulation of LBs in Stargardt's disease precedes macular degeneration (13). Mice carrying null mutations in *Abca4* and *Rdh8* develop blindness, basal laminar deposits, and focal accumulations of extracellular debris between the RPE and the Bruch membrane (drusen) (6).

Here we report that a family of modified cyclic oligosaccharides, beta cyclodextrins (β-CDs), formed by seven D-glucose units, can encapsulate the hydrophobic arms of A2E within their nonpolar cavity, protect A2E from oxidation, and remove A2E from RPE cells. Our data demonstrate a direct correlation between the ability of β-CDs to perform these protective functions and their affinity for A2E.

Results

β-CDs Protect A2E Against Fluorescence Quenching by Water. Because of conjugated double bonds in its hydrophobic arms, A2E exhibits a yellow–orange fluorescence with an emission peak at ~630 nm (λ_{max}) (14–16). Several studies indicate that A2E's λ_{max} changes with the polarity of the medium (17–19). To characterize better these polarity-related spectral changes, we compared the fluorescence spectrum of A2E in water and in several organic solvents. An increase in the polarity of the medium was accompanied by a shift to longer wavelengths in the λ_{max} and a reduction in the fluorescence intensity (height of the peak), which was very significant in water (Fig. S1).

This robust fluorescence quenching by water allowed us to screen for molecules capable of forming complexes that shield-off A2E from its aqueous environment. Based on the reported uses of cyclodextrins (CDs) as vehicles for drug delivery and as agents that encapsulate cholesterol and remove it from lysosomes in Niemann–Pick disease (20, 21), we investigated the

Significance

Lipofuscin accumulation in the retinal pigment epithelium (RPE) is a hallmark of aging. High lipofuscin levels in the RPE have been associated with retinal degeneration and blindness in Stargardt disease patients and animal models. Currently, there is no treatment to prevent and/or revert lipofuscin-driven retinal degenerative changes. In this study, we report that beta cyclodextrins, cyclic sugars composed of seven glucose units, can bind retinal lipofuscin, prevent its oxidation and remove it from RPE. This study opens an avenue to develop small drugs against, currently untreatable, lipofuscin-associated blinding disorders.

Author contributions: M.M.N., G.L.L., A.E.P.B., R.A.R., M.S., F.R.M., and E.R.-B. designed research; M.M.N., G.L.L., A.E.P.B., R.A.R., Z.J., S.G., and J.S. performed research; R.S., J.D.W., S.A.d.B., M.M., M.S., and F.R.M. contributed new reagents/analytic tools; M.M.N., G.L.L., A.E.P.B., R.A.R., Z.J., F.R.M., and E.R.-B. analyzed data; and M.M.N. and E.R.-B. wrote the paper.

Conflict of interest statement: A patent application has been submitted by Cornell, but not issued, concerning the use of cyclic oligosaccharides in lipofuscin removal. E.R.B. and M.M.N. are listed on this patent.

This article is a PNAS Direct Submission. J.R.S. is a guest editor invited by the Editorial Board.

[1]To whom correspondence may be addressed. E-mail: boulan@med.cornell.edu or mnociari@med.cornell.edu.

This article contains supporting information online at www.pnas.org/lookup/suppl/doi:10.1073/pnas.1400530111/-/DCSupplemental.

ability of CDs to bind A2E and remove it from RPE cells. CDs are a family of small cyclic D-glucose oligosaccharides. Naturally occurring CDs have rings composed of 6 (α-CD), 7 (β-CD), or 8 (γ-CD) glucose residues, with a hydrophilic exterior and a variably sized hydrophobic cavity. We found that, relative to water (black symbols), β-CD (red symbols) caused a blue-shift in the λmax of A2E's emission spectrum and an increase in its fluorescence intensity (Fig. 1*A*). In contrast, α-CD (green symbols) did not cause a significant λmax shift or enhancement, whereas γ-CD (blue symbols) elicited an intermediate response (Fig. 1*A*). The low ability of α- and γ-CDs to combine with A2E could not be overcome by increasing CD concentrations (Fig. 1*B*). Because methyl β-CD (Mβ-CD) remains soluble at much higher concentrations than the upper solubility limit of β-CD (12 mM) and is equally potent (Fig. 1*B*), all subsequent experiments were carried out using Mβ-CD.

β-CDs Protect A2E Against Oxidation. The absorption spectrum of A2E exhibits two absorbance maxima, at 340 and 440 nm, that correspond to the conjugated double bonds in the short and long arms of the molecule, respectively (14). In aqueous solution, A2E undergoes slow spontaneous oxidation manifested by progressive reduction of its absorbance peaks; upon exposure to blue light (~430 nm) the oxidative destruction of A2E is much faster (22, 23). The extent of oxidative destruction of A2E can be measured because, for every double bond oxidized, there is a ~30-nm blue shift in the absorbance maximum of the corresponding A2E arm (15, 16) (Fig. S2). β-CDs protected A2E against both photooxidation and spontaneous oxidation; interestingly, α-CD had no protective effect, whereas γ-CD had intermediate effects (Fig. 2 *C* and *D*).

Our experiments support a scenario in which the ability of CDs to protect against both spontaneous oxidative and photo-oxidative destructions of A2E is related to the size of their rings. The protection against oxidation correlates very well with the fluorescence enhancement by the various CDs.

Molecular Modeling of the A2E–CD Interaction. The size-dependent protection provided by CDs against both fluorescence quenching and oxidative destruction of A2E suggested that β-CD and to a lesser extent γ-CD, but not α-CD, might form inclusion complexes with A2E. To test this hypothesis, we carried out computational modeling of the interaction of A2E with the three CDs. Modeled molecules were energy minimized with MacroModel 9.9 using the OPLS 2005 force field in aqueous solution (24). As illustrated in Fig. 3*A*, this analysis predicted that α-, β-, and γ-CDs have cone-shaped inner cavities with diameters at the narrow end of 5.6, 6.8, and 8.0 Å, respectively, and that the terminal β-ionone rings at the end of both A2E arms are 6.5 Å in diameter. These calculations suggest that β-CD and γ-CD, but not α-CD, can accommodate the hydrophobic arms of A2E within their hydrophobic cavity. Consistent with this assumption, our calculations showed that the total energy of α-CD complexed with the short and long A2E arms is very high (>30,000 kJ/mol). Taken together, our experimental and modeling data support the hypothesis that β-CD and γ-CD, but not α-CD, can form inclusion complexes with A2E.

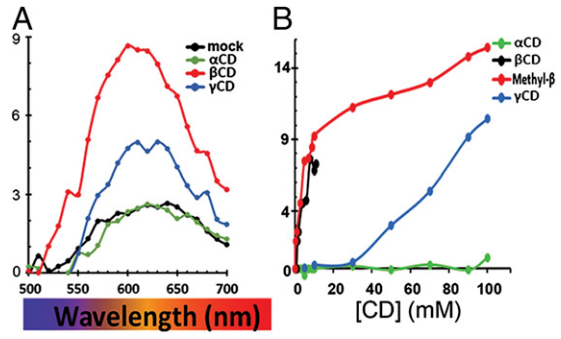

Fig. 1. Some CDs bind A2E. (*A*) Fluorescence spectra of A2E (black line) or A2E in the presence of 12 mM α-CD (green line), Mβ-CD (red line), and γ-CD (blue line) in aqueous solutions. (*B*) Dose–response changes in the fluorescence intensity of A2E (λex = 434 nm, λem = 610 nm) at increasing concentrations of α-, β-, Mβ-, and γ-CDs.

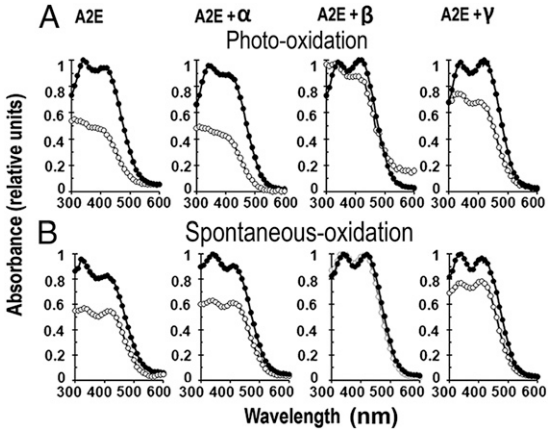

Fig. 2. Some CDs protect A2E against oxidation. Protection was monitored by changes in the UV-visible absorption spectra of 5 μM A2E solutions. (*A*) A2E oxidative status before (●) and after (○) blue-light irradiation in the presence of indicated cyclodextrins (12 mM). (*B*) A2E oxidative status at time 0 (●) and 1 d (○) after incubation at room temperature in the dark in the presence of cyclodextrins.

To gain further insights on the strength of the inclusion complex formed between β-CD and γ-CD with A2E, we estimated the dissociation constant using steady-state fluorescence measurements. Briefly, we monitored the incremental changes in A2E fluorescence ($F - F0$) with increasing CD concentrations [CD] and analyzed the data using the Benesi–Hildebrand double inverse plot. The dissociation constant (K_d) was estimated from the ratio between the slope and the intercept and was found to be 4 mM for β-CD and 365 mM for γ-CD (Fig. 3*B*; refs. 25 and 26).

Next, we prepared molecular models of the interactions between β-CDs and A2E by translating and rotating the β-CDs to form a complex with each chain of A2E, while minimizing steric clashes and considering water effects with MacroModel 9.9 using the OPLS 2005 force field. According to this model, A2E and related lipid bisretinoids are bivalent substrates. The results, shown in Fig. 3*C*, indicate that one β-CD encapsulates each hydrophobic arm of A2E snugly, as "a ring on a finger." Pioneering studies by Breslow and others have shown that dimeric cyclodextrins that interact simultaneously with both arms of bivalent ligands have lower dissociation rates (K_d) than monomeric CDs (27). Based on these studies and our own modeling data, we predicted that dimeric β-CDs with the β-CD monomers separated by a space equal to the distance between the tips of the A2E arms would interact with A2E with higher affinity than β-CD monomers. To test this prediction, we synthesized β-CD dimers with the two β-CD rings kept together by a linker as long as the distance between the tips of the A2E arms (Fig. 3*D*) and measured the affinity of their interaction with A2E comparatively with that of β-CD monomers, using the fluorescence assay described earlier. We estimated that the affinity of the β-CD dimer for A2E was about fourfold higher than that of the β-CD monomer ($K_d \sim 1$ vs. $K_d \sim 4$ mM, respectively; Fig. 3, *Inset*).

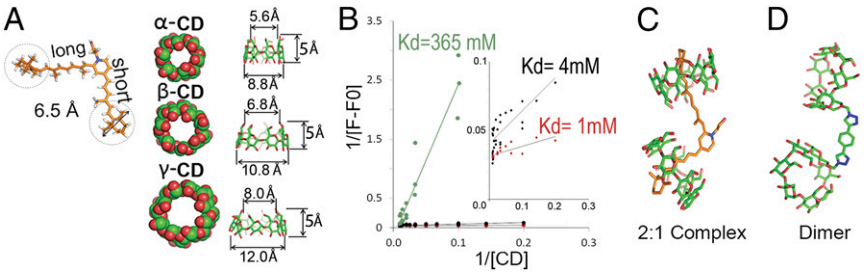

Fig. 3. Characterization of the interaction between A2E and CDs. (*A*) In scale, representation of A2E and CDs. A2E's β-ionone bulky head groups are marked with dotted circles. Major and minor interior cavity diameters of α-, β-, and γ-CDs are indicated. (*B*) Benesi–Hildebrand double inverse plot constructed with fluorescence data of A2E in presence of variable amounts of β-CD monomer (black), dimer (red), and γ-CD (green). (*Inset*) A zoomed view of the monomer (black) and dimer (red) plots. (*C*) Molecular modeling of the 2:1 β-CD:A2E complex. (*D*) β-CD-dimer synthesized to test the bivalent nature of β-CD:A2E interaction.

The computer modeling data and biochemical experiments discussed above provide strong supporting evidence for a scenario in which the protection of A2E by β-CDs from fluorescence quenching and oxidation depends on the ability of β-CD to snugly encapsulate the hydrophobic arms of A2E within its hydrophobic cavity. This model explains why α-CD, with a smaller cavity that cannot accommodate A2E arms, does not provide protection and why γ-CD, with a much larger cavity than A2E arms provides only limited protection. This model also explains why β-CD dimers can interact with higher affinity with A2E than β-CD monomers.

β-CDs Remove A2E from ARPE-19 Cells in Culture. The experiments discussed above suggest that β-CDs might also be capable of reducing cellular levels of A2E. Indeed, CDs are known to enter cells through endocytic routes leading to the lysosome (21, 28), and it has been shown that treatment with β-CDs can reduce lysosomal levels of cholesterol, another lipid that can form inclusion complexes with β-CD (29). As A2E deposits accumulate within lysosomes of RPE cells, we predicted that addition of β-CD to the medium might reduce A2E deposits in cultured RPE cells. To test this prediction, we loaded A2E into the lysosomal compartment of human RPE cells by adding medium supplemented with 10 μM A2E to the apical side of confluent and fully polarized monolayers of ARPE-19 cells grown on Transwell^{R} chambers. This protocol has been shown to result in lysosomal levels of A2E comparable to those present in RPE in normal human eyes (30). To mimic the physiological scenario, where nutrients access RPE cells from the choroidal side, we treated the RPE monolayers grown on Transwells with 500 μM Mβ-CD added to the basolateral side only. Treatment was done for 48 h with multiple changes of the medium. The amount of A2E remaining in RPE cells after CD treatment was determined by quantitative fluorescence microscopy and high-performance liquid chromatography (HPLC). Fig. 4*A* shows that A2E accumulated in the cytoplasm of RPE cells with a punctate pattern (consistent with lysosomes) and that the amount of A2E in the cells was highly reduced upon Mβ-CD treatment. Quantification of cytoplasmic A2E fluorescence in randomly selected fields from three independent experiments demonstrated that Mβ-CD treated cells displayed a 49% reduction in A2E fluorescence that was statistically significant ($P < 0.001$) (Fig. 4*B*). Detailed analysis of A2E-loaded ARPE-19 cells grown on glass bottom plates, using a 63× objective showed that A2E granules decreased in number and intensity upon treatment with Mβ-CD but not upon treatment with α-CD or γ-CD (Fig. S3*A*). Furthermore, other control experiments showed that β-CDs did not reduce the cell content of ceroid lipofuscins, the type of lipofuscin found in neurons and cardiomyocytes, indicating that the observed removal by Mβ-CD is highly specific for bisretinoid-containing lipofuscins (Fig. S3*B*).

Consistently with the microscopy data, HPLC quantification revealed a ∼70% reduction ($P < 0.001$) in the total A2E levels in Mβ-CD–treated cells (Fig. 4*C*). The 20% higher removal estimated by HPLC compared with quantitative fluorescence microscopy suggests that the optical quantification method underestimates A2E removal, perhaps because the remaining A2E would fluoresce more upon interaction with CD (Fig. 1).

In summary, these experiments demonstrate that basolateral exposure to Mβ-CD of RPE monolayers preloaded with A2E drastically reduces lysosomal A2E deposits.

β-CDs Remove LBs from Mouse RPE ex Vivo. To answer whether Mβ-CD can also effectively reduce the mix of LBs that naturally accumulates in the lysosomes of the RPE in the eye, we carried out ex vivo and in vivo experiments with *Abca4-Rdh8* double knockout (DKO) animals. These mice accumulate A2E rapidly and develop early onset blindness, basal lamina deposits, and drusen (6).

First, we tested the ability of Mβ-CD to reduce LBs from DKO mouse eyes ex vivo. To this end, eyes from 6-mo-old DKOs were

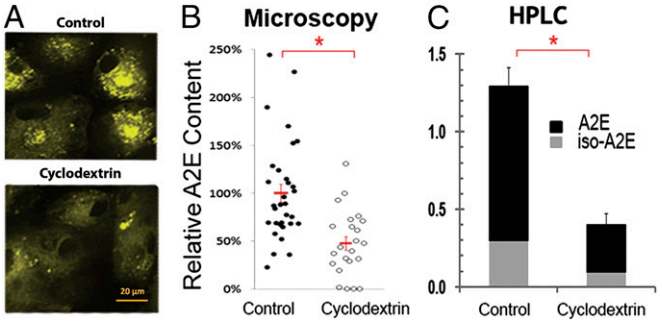

Fig. 4. Basolateral Mβ-CD reduces A2E levels in fully polarized RPE monolayers. Polarized ARPE-19 cultures on Transwells, were O/N preloaded with A2E, cultured for 3 d in media and exposed through the apical side to vehicle (control) or 500 μM Mβ-CD (treated) from the basal side for 48 h with several changes of medium. (*A*) Representative confocal fluorescence image. Note the punctate staining pattern corresponding to the accumulation of A2E in lysosomes and the reduction after treatment with Mβ-CD. (*B*) Quantification of the A2E fluorescence levels by fluorescence microscopy. Data points, obtained from three separate experiments, represent relative mean fluorescence intensity from randomly selected fields after background subtraction. Treatment with Mβ-CD resulted in a 49% decrease in A2E fluorescence, relative to mock treated cells ($P < 0.001$). (*C*) Quantification of A2E levels by HPLC. Treatment with Mβ-CD resulted in 73% extraction of both A2E and iso-A2E ($n = 4$, $P < 0.001$).

enucleated; cornea, lens, and other anterior structures were eliminated by coronal sectioning; and neural retinas were removed under conditions of minimal adherence (*Methods*). Eyecups with the exposed RPE were then incubated in the presence of medium supplemented with 500 μM Mβ-CD for 3 d, with multiple changes of the medium in between. For scanning fluorescence microscopy, eyecups were fixed with 4% PFA, flat mounted and counterstained with Phalloidin-Alexa Fluor 680 (actin filaments) and DAPI (nuclei). Fig. 5*A* shows the granular appearance of LBs in control RPE obtained from *Abca4-Rdh8* DKO mice, consistent with their accumulation in lysosomes. Note that upon treatment with Mβ-CD, the number and intensity of lipofuscin granules are reduced. Fig. 5*B* shows the quantification of LB fluorescence levels in randomly selected fields of treated versus control eyecups from three independent experiments. By this method, the estimated reduction in LB fluorescence caused by Mβ-CD was over 31% ($P < 0.0007$).

To confirm this result using an independent experimental approach and to quantitatively characterize the effect of Mβ-CD treatment on the different types of bisretinoids accumulated in the RPE of DKO retinas, we carried out HPLC analysis of mouse eyecup chloroform extracts using methods described in ref. 31. To this end, seven 6-mo-old DKO mice were killed, and their right and left eyes' eyecups were treated for 72 h with media (control) and 500 μM Mβ-CD (experimental), respectively. The graph shown in Fig. 5*C* is an overlay of representative HPLC chromatograms of an age-matched control (black trace) and Mβ-CD–treated eyecup (red trace). The identity of the peaks was assessed by online spectral analysis against previously established peaks obtained by elution with standards. As depicted, Mβ-CD was effective at reducing the levels of all detectable bisretinoids, including A2E, A2E isomers (iso-A2E#1, #2, #3), A2E precursors (dihydro-A2PE (A2PE-H_2) and A2PE), as well as all-*trans*-retinaldehyde dimer (atRAL-dimerPE). In contrast, the level of *N*-Ret-PE, the monoretinoid precursor of A2E, was unperturbed by the treatment suggesting monomeric ligands need higher local CD concentrations for effective removal. For each eye, the amount of total A2E was calculated as the sum of A2E and iso-A2E peaks. The results are plotted in Fig. 5*D*. The mean and SE for controls and treated eyes are indicated in red. The average Mβ-CD–mediated total A2E reduction was higher than 48% ($P < 0.005$). The average calculated changes for the other retinoids were: 46% ($P < 0.05$) for A2PE, 30% ($P < 0.02$) for A2PE-H_2, 25% ($P < 0.04$) for atRAL-dimerPE, and 8% ($P > 0.24$) for *N*-Ret-PE.

β-CDs Remove LBs from Mouse RPE in Vivo. Next, we tested the ability of Mβ-CD to remove LBs from DKO mice eyes in vivo. To this end, eight 9-mo-old DKO mice received in their right eyes 1.5 μL of 100 mM Mβ-CD in PBS through intraocular injections every other day four times as depicted in Fig. 6*A*. The left eyes were identically injected with PBS to serve as controls. At day nine the animals were killed and the right and left eyes were enucleated, the neural retina removed and the eyecups were analyzed for bisretinoid content using HPLC. As shown in Fig. 6*B* the total content of A2E, (i.e., A2E plus iso-A2E) was ~25% lower in the treated right eyes relative to the control left eyes.

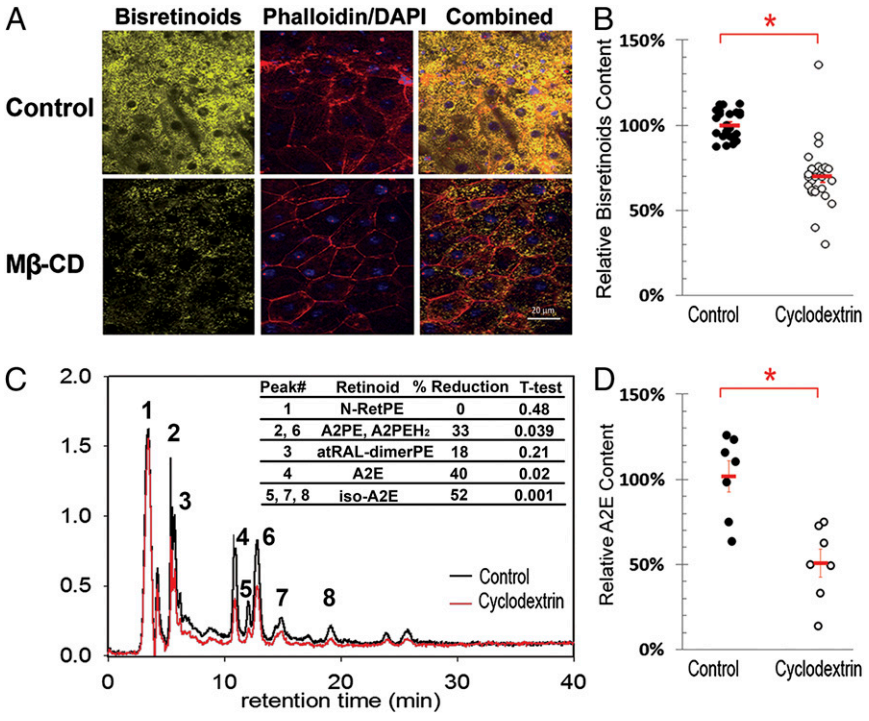

Fig. 5. Mβ-CD removes LBs from *Abca4-Rdh8* DKO eyes ex vivo. (*A*) Flat mounted eyecups from *Abca4-Rdh8* mice after 72 h incubation in culture media alone (control) or supplemented with 500 μM Mβ-CD. RPE borders and nuclei were labeled with phalloidin (red) and DAPI (blue), respectively. Auto fluorescent LB granules are in yellow. (*B*) Quantification of lipofuscin's mean fluorescence intensity per randomly chosen field in controls ($n = 3$) and Mβ-CD treated ($n = 3$) eyecups. Means ± SEM of the three experiments are in red. The attained reduction in bisretinoid fluorescence was 31% ($P < 0.0007$). (*C*) Representative HPLC chromatogram showing the bisretinoids profile of control (black trace) and Mβ-CD-treated (red trace) eyecup extracts. The inserted table depicts the average reduction of the areas under the peaks for all identified retinoids ($n = 7$ control eyes and 7 treated eyes). All identified peaks show reduction. In addition, there are some minor unidentified peaks that also show reduction; they likely correspond to small amounts of oxidized bisretinoids. (*D*) Quantitation by HPLC of total A2E. Individual dots represent the total content of A2E (A2E plus iso-A2E) per eyecup. Seven age-matched eyecup extracts from *Abca4-Rdh8* DKO mice for each group, control (black) and Mβ-CD-treated (open) are presented in the graph. The average content and SE for controls and Mβ-CD treated eyecups are indicated in red. The difference corresponds to a reduction of 48% ($P < 0.005$).

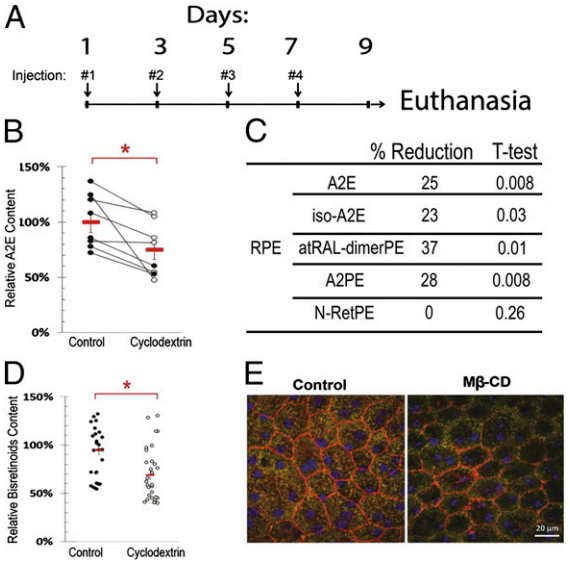

Fig. 6. Intravitreal Mβ-CD reduces LB in the RPE of *Abca4-Rdh8* DKO mice. (*A*) Schematic diagram of intravitreal injections and euthanasia. Right (treated) and left (controls) eyes received 1.5 μL of 100 mM Mβ-CD in PBS and PBS, respectively, in each administration. Eye specimens were analyzed by HPLC and Microscopy. (*B*) Difference in the content of total A2E (A2E and iso-A2E) between left (control) and right (cyclodextrin) eyes determined by HPLC. Each dot represents one eye ($n = 8$). Red symbols are average content and SEs. The difference between eyes corresponds to a reduction of 24% ($P < 0.013$). (*C*) Differential content of bisretinoids and bisretinoid precursors in the RPE as determined by HPLC. (*D*) Quantification of the content of bisretinoids in the left and right eyes by quantitative fluorescence microscopy. The difference between eyes corresponds to 27% ($P < 0.01$). (*E*) Representative inmmunofluorescence of flat mounted eyecups depicting the integrity of the RPE layer. CD treatment reduced the number and fluorescent intensity of lipofuscin granules. Actin filaments at cell borders (red) and nuclei (blue) were decorated with phalloidin and DAPI, respectively. All panels are at the same magnification (×400).

Similar to what we observed in the ex vivo experiments, the treatment with Mβ-CD also reduced significantly the levels of other bisretinoids. Thus, atRAL-dimerPE and A2PE were reduced 37% and 28% in the RPE (Fig. 6*C*). Fig. 6*D* shows the level of LBs in random fields, in control and treated eyes, determined by quantitative fluorescence microscopy; these data are in full agreement with the HPLC data.

Importantly, RPE cells appear to tolerate well the CDs treatment with the protocol used. Immunofluorescence analysis of flat mounted eyecups using Phalloidin and DAPI to delineate the cellular borders and nuclei, respectively, show that RPE cells in the CD-treated eye have normal size and histologic appearance and that the effect of the CD was mainly reducing the number and intensity of the LB granules (Fig. 6*E*).

In summary, these experiments demonstrate that treatment with Mβ-CD effectively reduces cellular levels of bisretinoids, including A2E, that have been accumulated in the lysosomes of RPE cells through natural mechanisms, without noxious effects on the RPE.

Discussion

The primary goal of this study was to develop a method to reduce the deposits of LBs in *Abca4-Rdh8* DKO mice, an animal model that mimics human Stargardt's disease and shows pathological signs of age-related macular degeneration (AMD). Because single mutant *Abca4*$^{-/-}$ mice accumulate significant LB granules in the RPE but show normal retinal function (7) and all-trans-retinal-aldehyde (atRAL) is more toxic than LBs in culture (32), it has been proposed that A2E and other condensation products are just surrogate markers of aberrant atRAL clearance that form to minimize the toxicity of free atRAL (33–35). However, there is no doubt that LBs are also toxic to the RPE. Both, Boulton and Sparrow's laboratories have reported a phototoxic effect of A2E upon exposure to blue light (15, 36). Accumulation of A2E leads to plasma membrane destabilization (17, 19, 37), increased lysosomal pH (38–40), decreased lysosomal enzyme activity (39), and derailing of cholesterol trafficking with the consequent buildup of free cholesterol in lysosomes (41). Moreover, accumulation of LBs in RPE is known to induce complement activation (42, 43) and secretion of proinflammatory cytokines, including IL-1β, IL-8, IL-6, VEGFα, TNFa, and chemokines (44–46) responsible, at least in part, for the perpetuation of the chronic inflammatory milieu linked with AMD (47, 48). Hence, irrespectively of how much atRAL or LBs contribute to the retinal degenerative process in the young, we expect that the steady and prolonged accumulation of LBs will progressively weigh more on this balance and therefore, the removal of LBs should have a beneficial impact, particularly, for the elderly retinas. Thus, searching for new strategies to reduce A2E and other condensation products in RPE is an important medical goal. As a first step in this direction, we identified molecules, the β- and γ-CDs, that bind to A2E.

Additional insights on the interaction between CDs and A2E were provided by the demonstration that they can protect A2E against spontaneous oxidative and photooxidative degradation (Fig. 2). Oxygen attack of the double bonds in A2E's hydrophobic arms permanently destroys A2E's ability to fluoresce. The initial oxidative events can occur via light-independent (spontaneous) or light-dependent (photo-) oxidative reactions (3). Spontaneous oxidation occurs in the absence of light and is thought to be mediated by free-radical chain reactions (23, 49). Photooxidation of A2E, on the other hand, is most efficiently triggered by wavelengths in the blue range (430 nm) and is believed to occur through double-bond isomerization and nonradical singlet oxygen generation that causes self-oxidation (10, 50). Both types of oxidative cascades ultimately lead to degradation of bisretinoids into small, highly reactive carbonyls. In turn, these reactive oxygen species cross-link (bio) molecules, through Michael addition or Schiff base reactions that cannot be stopped by antioxidants (37, 51). β-CDs prevented both photooxidative (Fig. 2*A*) and spontaneous oxidative (Fig. 2*B*) cascades, suggesting that they protect bisretinoids against both singlet oxygen and free radical attacks. This protection of A2E against oxidation recapitulates the protection previously described against water quenching, i.e., β-CD> γ-CD>> α-CD, suggesting that β-CDs have a better suited cavity to encapsulate A2E.

Using computational modeling, we found that the hydrophobic cavities of α-CDs/γ-CD are too narrow or too wide to accommodate snugly the A2E arms, whereas the hydrophobic cavity of β-CD is just the right size (Fig. 3*A*). We estimated that the equilibrium constants (K_d) of the inclusion complexes between A2E and β-CD or γ-CD are ∼4 mM and 365 mM, respectively (Fig. 3*B*). The higher K_d for γ-CD agrees with a looser fit with the arms of A2E, which is supported by its ability to offer only mediocre protection against quenching and oxidation. Computer modeling of the inclusion complexes reinforced this notion and furthermore predicted that CD dimers with a mirror configuration to the two hydrophobic arms of the "V" shaped A2E molecule (which diverge with an angle of 101°) might bind A2E with higher selectivity (Fig. 3*C*). This prediction was supported by data published by Breslow and coworkers (27), who demonstrated that CD-dimers with a configuration complementary to a V-shaped ligand displayed higher affinity for the ligand than the corresponding CD monomer. To experimentally test this prediction, we synthesized a β-CDs dimer with a configuration complementary to A2E and

showed that, indeed, this molecule displayed higher affinity for A2E (Fig. 3 *B* and *D*).

The interaction we observed between β-CD and A2E encouraged us to study whether β-CD treatment would be capable of reducing A2E levels in RPE. Indeed, β-CD applied in culture effectively reduced A2E/bisretinoid levels in ARPE-19 (Fig. 4) and eyecups (Fig. 5). The CDs most effective in reducing cellular A2E were those most effective at forming complexes with A2E (Fig. S3*A*). Moreover, β-CD's specifically depleted retinoid conjugates with similar bivalent hydrophobic structure, i.e., A2E, iso-A2E, A2PE, A2PE-H_2, and atRAL-dimer PE (Fig. 5*C*), yet were ineffective decreasing the monovalent *N*-Ret-PE as well as ceroid lipofuscin deposits from RPE cells (Fig. 5*C* and Fig. S3*B*). Next, we investigated the removal ability of β-CDs in vivo. As shown in Fig.6, local intravitreal administration of Mβ-CD was similarly efficacious to reduce the LB deposits in the RPE of old *Abca4-Rdh8* DKO mice with no visible toxic side effects on these cells, according to histological examination (Fig. 6*E*). Further studies are needed to determine whether reduction of LB levels can prevent and reverse loss of visual acuity in young and old *Abca4-Rdh8* DKO animals, respectively.

At this point, we can only speculate on the mechanisms involved in the CD-mediated clearance of A2E and other bisretinoids from RPE cells. The best characterized related property of β-CDs (i.e., their ability to extract lysosomal cholesterol from fibroblasts from Niemann–Pick patients) appears to be related to their capability to enter lysosomes via endocytosis (28, 52) and their presumed role in facilitating delivery of unesterified cholesterol to the limiting lysosomal membrane for transfer elsewhere in the cell (21, 28). Lysosomal β-CDs could similarly solubilize A2E and facilitate its mobilization outside the cell or into catabolic organelles. Additional research is needed to elucidate the mechanisms involved in β-CD–induced lysosomal clearance of LBs.

β-CDs have been reported to improve neuropathological conditions associated with the lysosomal accumulation of cholesterol, such as Niemann–Pick type C (53, 54) and Alzheimer's disease (55). Our results suggest that β-CDs can have an effect on LB-driven retinal degeneration. However, their use in vivo imposes that β-CDs should be nontoxic and be able to maintain high concentrations in the eye's RPE. Although there are β-CDs that have been already approved by the FDA as Investigational New Drugs, their fast renal clearance and low efficiency to reach the back of the eye precludes their immediate application. The experiments reported here suggest potential avenues to optimize CDs (i.e., facilitating their lysosomal uptake via specific lysosomal uptake receptors) and creating CDs with higher affinity for A2E (e.g., by generating the appropriate dimers). An improved understanding of the cellular A2E-reduction mechanisms will also provide a rational basis to develop more efficient CD-based in vivo treatments.

Materials and Methods

Reagents. α-CD, β-CD, Mβ-CD (332615), γ-CD, Ethanol, Ethyl Acetate, Toluene, and Hexane were all purchased from Sigma. Cyclodextrin stock solutions were prepared at 100 mM in PBS buffer (pH 7.2) except for β-CD system, which, due to the insolubility, was dissolved at 12.5 mM.

Steady-State Fluorescence and Absorption Spectroscopy. Fluorescence and absorption spectra of A2E in organic solvents or aqueous solutions of CDs were recorded in a thermally controlled SpectraMax M2 (Molecular Devices) using quartz cuvettes and 96-well, dark wall/clear bottom plates. For all polarity-shift measurements, A2E was used at 5 μM. For photooxidation assays, samples were irradiated in uncapped Eppendorf tubes for 5 min with a 450 ± 20 nm 90 Blue-LEDs light source (90 Watts, 1,980 Lumen) at a distance of ∼8 cm from the top of the tubes. To measure the photostability of the A2E in CDs, A2E–CD complexes were allowed to form for 1 h before blue-light exposure. For spontaneous oxidation experiments, samples in foil-wrapped screw capped glass tubes, were incubated at room temperature for the indicated times before spectroscopic analysis.

For the determination of the A2E/CD complex equilibrium constant, a series of seven twofold CD-dilutions were prepared in which the A2E concentration was identical (5 μM) and the CD concentration was varied from 0 to 100 mM. Fluorescence of the complexes was measured using 434 nm for excitation and 600 nm for detection. The dissociation constant (K_d) was calculated as the ratio between the slope and intercept from the $1/(F - F0)$ vs. $1/[CD]$ double inverse plot.

Eyecups Preparation and CD Treatment. For in vivo extraction of LBs, posterior eyecups were prepared from 6-mo-old *Abca4-Rdh8* DKO mice in optimized conditions to preserve RPE apical structures during sample preparation. Briefly, animals were maintained in complete darkness for 48 h, the eyes enucleated 2 h after the end of the dark cycle (8:00 PM) and placed immediately in $Ca^{2+}Mg^{2+}$ free-HBSS (CMF HBSS). The lens and vitreous were removed and the eyes incubated for 30 min in CMF HBSS until spontaneous retinal detachment. To prepare RPE eyecups, the retina was excised from the optic nerve and the eyecups were everted to maximize RPE exposition to the culture media and prevent self-folding under suspension. Eyecups were treated with medium supplemented with 500 μM Mβ-CD for three days, replacing the media every day.

Lipofuscins Synthesis and Loading. A2E was synthesized and purified by HPLC (>97%) according to a published protocol (17). Ceroid lipofuscin was prepared by oxidative cross-linking of mitochondrial and lysosomes as described (56). Loading of A2E and ceroid lipofuscins into ARPE-19 cells was done by adding 10 μM A2E (MW:592) or 15 mg/mL ceroid lipofuscin for 6 h. Fully polarized monolayers received lipofuscin through their apical side. Cells were then washed and chased for 5 d in fresh media.

Cell Cultures and CD Treatments. Cells were incubated with media supplemented with 500 μM of the indicated CD for 48 h with 12 replacements of media during that period. Fully polarized ARPE-19 cells received the CD media only through their basolateral side to reproduce the removal although the back of the eye.

In Vivo CD Treatment. *Abca4-Rdh8* DKO mice (6 mo old) were anesthetized by i.p. injection of ketamine (100 mg/kg) and xylazine (10 mg/kg). The cornea was further anesthetized topically with one drop of 0.5% proparacaine hydrochloride for 2 min and the pupils dilated with a topical instillation of 0.5% tropicamide and 2.5% phenylephrin. The intravitreal injection was performed under magnification of an ophthalmic surgical microscope (model M841; Leica, Wetzlar, Germany) with a 34 gauge beveled needle attached to a 10 μL syringe of a Nanofil injection system (World Precision Instruments) controlled by a microprocessor-based microsyringe pump controller (Fusion 200 Syringe Pump, Chemyx). The needle was introduced through the sclera 1 mm posterior to limbus into the vitreous chamber of the eye, and 1.5 μL of either 100 mM Mβ-CD (right eye) or PBS (left eye) was slowly injected. A 30-s interval was kept before removing the needle to prevent backflow. The animals were treated with antibiotic eye ointment (Moxifloxacin; Alcon Laboratories) and maintained at 37 °C until anesthesia recovery. During the entire procedure, mice were kept in the dark and received a total of four injections per eye, every 2 d; mice were killed at day 9. All animal procedures were performed according to the regulations in the Association for Research in Vision and Opthalmology Statement for the Use of Animals in Ophthalmic and Vision Research and were approved by the local ethics committee.

HPLC Analysis of Bisretinoids Content. Bisretinoids were extracted from mouse eyecups and polarized ARPE-19 filters cells under red dim light. Briefly, single mouse eyecup (containing RPE/choroid/sclera, devoid of neural retina) or ARPE-19 cells were washed with phosphate buffer (PBS) and homogenized in 1 mL of PBS. Four milliliters chloroform/methanol (2:1, vol/vol) was added, and the samples were extracted with the addition of 4 mL of chloroform and 3 mL of dH2O, followed by centrifugation at 1,000 × *g* for 10 min. Extraction was repeated with the addition of 4 mL of chloroform. Organic phases were pooled, filtered, dried under a stream of argon, and redissolved in 100 μL of 2-propanol. Bisretinoid extracts were analyzed by normal-phase HPLC with a silica column (Zorbax-Sil 5 μm, 250 × 4.6 mm; Agilent Technologies) as described (31). The mobile phase was hexane/2-propanol/ethanol/25 mM potassium phosphate/glacial acetic acid (485:376:100:45:0.275 vol/vol) and was filtered before use. The flow rate was 1 mL/min. Column and solvent temperatures were maintained at 40 °C. Absorption units at 435 nm were converted to picomoles using a calibration curve with an authentic A2E

standard and the published molar extinction coefficient for A2E; the identity of each bisretinoid peak was confirmed by online spectral analysis.

Computational Modeling. Structures of CD were taken from the Protein Data Bank (PDB): α-CD (PDB ID code 2XFY), β-CD (PDB ID code 1DMB), and γ-CD (PDB ID code 1P2G). The 3D structure of A2E was built with Maestro 9.2 (Schrödinger). All structures were minimized in water with MacroModel 9.9 using the OPLS 2005 force field, for 500 steps of conjugate gradient minimizations. Complexes of α-, β-, or γ-CD and A2E were prepared manually by translating and rotating CD to form a complex with each chain of A2E while minimizing steric clashes. Energy calculation: energies for CD–A2E complexes were calculated with MacroModel 9.9 using the OPLS 2005 force field.

Synthesis of Dimeric β-CD. Details on the synthesis are provided in *SI Materials and Methods* and Fig. S4.

ACKNOWLEDGMENTS. We thank Krzyzstof Palczewski (Case Western Reserve University) for providing *Abca4-Rdh8* DKOs, Dr. Harel Weinstein (Weill Cornell Medical College) for molecular modeling and comments on the manuscript, and Kevin Lazo for his technical help. This work was supported by the Beckman, Research to Prevent Blindness, and Dyson Foundations; National Institutes of Health Grants EY022165 and EY08538 (to E.R.B.); and a Clinical Translational Scientific Center Pilot Award and a Macular Degeneration Research Standard Award from the Bright Focus Foundation (to M.M.N.). G.L.L. was supported in part by a Pew International Postdoctoral Fellowship.

1. Strauss O (2005) The retinal pigment epithelium in visual function. *Physiol Rev* 85(3): 845–881.
2. Sparrow JR, Hicks D, Hamel CP (2010) The retinal pigment epithelium in health and disease. *Curr Mol Med* 10(9):802–823.
3. Sparrow JR, Boulton M (2005) RPE lipofuscin and its role in retinal pathobiology. *Exp Eye Res* 80(5):595–606.
4. Eldred GE, Lasky MR (1993) Retinal age pigments generated by self-assembling lysosomotropic detergents. *Nature* 361(6414):724–726.
5. Ng K-P, et al. (2008) Retinal pigment epithelium lipofuscin proteomics. *Mol Cell Proteomics* 7(7):1397–1405.
6. Maeda A, Maeda T, Golczak M, Palczewski K (2008) Retinopathy in mice induced by disrupted all-trans-retinal clearance. *J Biol Chem* 283(39):26684–26693.
7. Weng J, et al. (1999) Insights into the function of Rim protein in photoreceptors and etiology of Stargardt's disease from the phenotype in abcr knockout mice. *Cell* 98(1): 13–23.
8. Wu Y, Zhou J, Fishkin N, Rittmann BE, Sparrow JR (2011) Enzymatic degradation of A2E, a retinal pigment epithelial lipofuscin bisretinoid. *J Am Chem Soc* 133(4): 849–857.
9. Sparrow JR, Kim SR, Cuervo AM, Bandhyopadhyayand U (2008) A2E, a pigment of RPE lipofuscin, is generated from the precursor, A2PE by a lysosomal enzyme activity. *Adv Exp Med Biol* 613:393–398.
10. Schütt F, Davies S, Kopitz J, Holz FG, Boulton ME (2000) Photodamage to human RPE cells by A2-E, a retinoid component of lipofuscin. *Invest Ophthalmol Vis Sci* 41(8): 2303–2308.
11. Sparrow JR, Cai B (2001) Blue light-induced apoptosis of A2E-containing RPE: Involvement of caspase-3 and protection by Bcl-2. *Invest Ophthalmol Vis Sci* 42(6): 1356–1362.
12. Holz FG, Bellman C, Staudt S, Schütt F, Völcker HE (2001) Fundus autofluorescence and development of geographic atrophy in age-related macular degeneration. *Invest Ophthalmol Vis Sci* 42(5):1051–1056.
13. Allikmets R, et al. (1997) A photoreceptor cell-specific ATP-binding transporter gene (ABCR) is mutated in recessive Stargardt macular dystrophy. *Nat Genet* 15(3):236–246.
14. Washington I, Jockusch S, Itagaki Y, Turro NJ, Nakanishi K (2005) Superoxidation of bisretinoids. *Angew Chem Int Ed Engl* 44(43):7097–7100.
15. Kim SR, Jockusch S, Itagaki Y, Turro NJ, Sparrow JR (2008) Mechanisms involved in A2E oxidation. *Exp Eye Res* 86(6):975–982.
16. Jang YP, Matsuda H, Itagaki Y, Nakanishi K, Sparrow JR (2005) Characterization of peroxy-A2E and furan-A2E photooxidation products and detection in human and mouse retinal pigment epithelial cell lipofuscin. *J Biol Chem* 280(48):39732–39739.
17. Sparrow JR, Parish CA, Hashimoto M, Nakanishi K (1999) A2E, a lipofuscin fluorophore, in human retinal pigmented epithelial cells in culture. *Invest Ophthalmol Vis Sci* 40(12):2988–2995.
18. Ragauskaite L, Heckathorn RC, Gaillard ER (2001) Environmental effects on the photochemistry of A2-E, a component of human retinal lipofuscin. *Photochem Photobiol* 74(3):483–488.
19. De S, Sakmar TP (2002) Interaction of A2E with model membranes. Implications to the pathogenesis of age-related macular degeneration. *J Gen Physiol* 120(2):147–157.
20. Abi-Mosleh L, Infante RE, Radhakrishnan A, Goldstein JL, Brown MS (2009) Cyclodextrin overcomes deficient lysosome-to-endoplasmic reticulum transport of cholesterol in Niemann-Pick type C cells. *Proc Natl Acad Sci USA* 106(46):19316–19321.
21. Rosenbaum AI, Maxfield FR (2011) Niemann-Pick type C disease: Molecular mechanisms and potential therapeutic approaches. *J Neurochem* 116(5):789–795.
22. Ben-Shabat S, et al. (2002) Formation of a nonaoxirane from A2E, a lipofuscin fluorophore related to macular degeneration, and evidence of singlet oxygen involvement. *Angew Chem Int Ed Engl* 41(5):814–817.
23. Wang Z, Keller LMM, Dillon J, Gaillard ER (2006) Oxidation of A2E results in the formation of highly reactive aldehydes and ketones. *Photochem Photobiol* 82(5): 1251–1257.
24. Schurig HPNV (1990) Neue analytische Methoden: Gaschromatographische Enantiomerentrennung an Cyclodextrinderivaten (Gas chromatographic Separation of Enantiomers on Cyclodextrin Derivatives). *Angew Chem Int Ed Engl* 29:939–1076.
25. Benesi HA, Hildebrand JH (1949) A Spectrophotometric Investigation of the Interaction of Iodine with Aromatic Hydrocarbons. *J Am Chem Soc* 71:2703–2707.
26. Baker GA, Crane NJ, Mayrhofer RC, Betts TA (2002) Cyclodextrin Inclusion Complexes with a Solvatochromic Fluorescent Probe. *J Chem Educ* 79:1261.
27. Breslow R, Halfon S, Zhang B (1995) Molecular recognition by cyclodextrin dimers. *Tetrahedron* 51:377–388.
28. Rosenbaum AI, Zhang G, Warren JD, Maxfield FR (2010) Endocytosis of beta-cyclodextrins is responsible for cholesterol reduction in Niemann-Pick type C mutant cells. *Proc Natl Acad Sci USA* 107(12):5477–5482.
29. Mondal M, Mesmin B, Mukherjee S, Maxfield FR (2009) Sterols are mainly in the cytoplasmic leaflet of the plasma membrane and the endocytic recycling compartment in CHO cells. *Mol Biol Cell* 20(2):581–588.
30. Sparrow JR, Kim SR, Wu Y (2010) Experimental approaches to the study of A2E, a bisretinoid lipofuscin chromophore of retinal pigment epithelium. *Methods Mol Biol* 652:315–327.
31. Radu RA, et al. (2008) Accelerated accumulation of lipofuscin pigments in the RPE of a mouse model for *Abca4*-mediated retinal dystrophies following Vitamin A supplementation. *Invest Ophthalmol Vis Sci* 49(9):3821–3829.
32. Wielgus AR, Chignell CF, Ceger P, Roberts JE (2010) Comparison of A2E cytotoxicity and phototoxicity with all-trans-retinal in human retinal pigment epithelial cells. *Photochem Photobiol* 86(4):781–791.
33. Maeda A, et al. (2012) Primary amines protect against retinal degeneration in mouse models of retinopathies. *Nat Chem Biol* 8(2):170–178.
34. Maeda A, et al. (2009) Involvement of all-trans-retinal in acute light-induced retinopathy of mice. *J Biol Chem* 284(22):15173–15183.
35. Maeda T, Golczak M, Maeda A (2012) Retinal photodamage mediated by all-trans-retinal. *Photochem Photobiol* 88(6):1309–1319.
36. Godley BF, et al. (2005) Blue light induces mitochondrial DNA damage and free radical production in epithelial cells. *J Biol Chem* 280(22):21061–21066.
37. Sokolov VS, et al. (2007) Interaction of pyridinium bis-retinoid (A2E) with bilayer lipid membranes. *J Photochem Photobiol B* 86(2):177–185.
38. Baltazar GC, et al. (2012) Acidic nanoparticles are trafficked to lysosomes and restore an acidic lysosomal pH and degradative function to compromised ARPE-19 cells. *PLoS ONE* 7(12):e49635.
39. Holz FG, et al. (1999) Inhibition of lysosomal degradative functions in RPE cells by a retinoid component of lipofuscin. *Invest Ophthalmol Vis Sci* 40(3):737–743.
40. Jarrett SG, Boulton ME (2012) Consequences of oxidative stress in age-related macular degeneration. *Mol Aspects Med* 33(4):399–417.
41. Lakkaraju A, Finnemann SC, Rodriguez-Boulan E (2007) The lipofuscin fluorophore A2E perturbs cholesterol metabolism in retinal pigment epithelial cells. *Proc Natl Acad Sci USA* 104(26):11026–11031.
42. Zhou J, Kim SR, Westlund BS, Sparrow JR (2009) Complement activation by bisretinoid constituents of RPE lipofuscin. *Invest Ophthalmol Vis Sci* 50(3):1392–1399.
43. Ma W, Coon S, Zhao L, Fariss RN, Wong WT (2013) A2E accumulation influences retinal microglial activation and complement regulation. *Neurobiol Aging* 34(3): 943–960.
44. Anderson OA, Finkelstein A, Shima DT (2013) A2E induces IL-1ß production in retinal pigment epithelial cells via the NLRP3 inflammasome. *PLoS ONE* 8(6):e67263.
45. Holtkamp GM, et al. (1998) Polarized secretion of IL-6 and IL-8 by human retinal pigment epithelial cells. *Clin Exp Immunol* 112(1):34–43.
46. Iriyama A, et al. (2009) A2E, a component of lipofuscin, is pro-angiogenic in vivo. *J Cell Physiol* 220(2):469–475.
47. Buschini E, Piras A, Nuzzi R, Vercelli A (2011) Age related macular degeneration and drusen: Neuroinflammation in the retina. *Prog Neurobiol* 95(1):14–25.
48. Kanda A, Abecasis G, Swaroop A (2008) Inflammation in the pathogenesis of age-related macular degeneration. *Br J Ophthalmol* 92(4):448–450.
49. Girotti AW (1985) Mechanisms of lipid peroxidation. *J Free Radic Biol Med* 1(2):87–95.
50. Sparrow JR, et al. (2002) Involvement of oxidative mechanisms in blue-light-induced damage to A2E-laden RPE. *Invest Ophthalmol Vis Sci* 43(4):1222–1227.
51. Yoon KD, Yamamoto K, Ueda K, Zhou J, Sparrow JR (2012) A novel source of methylglyoxal and glyoxal in retina: Implications for age-related macular degeneration. *PLoS ONE* 7(7):e41309.
52. Plazzo AP, et al. (2012) Uptake of a fluorescent methyl-β-cyclodextrin via clathrin-dependent endocytosis. *Chem Phys Lipids* 165(5):505–511.
53. Vance JE, Peake KB (2011) Function of the Niemann-Pick type C proteins and their bypass by cyclodextrin. *Curr Opin Lipidol* 22(3):204–209.
54. Davidson CD, et al. (2009) Chronic cyclodextrin treatment of murine Niemann-Pick C disease ameliorates neuronal cholesterol and glycosphingolipid storage and disease progression. *PLoS ONE* 4(9):e6951.
55. Yao J, et al. (2012) Neuroprotection by cyclodextrin in cell and mouse models of Alzheimer disease. *J Exp Med* 209(13):2501–2513.
56. Nilsson E, Yin D (1997) Preparation of artificial ceroid/lipofuscin by UV-oxidation of subcellular organelles. *Mech Ageing Dev* 99(1):61–78.